



# A proximity tagging strategy utilizing an activated aldehyde group as the active site

Mengfan Zhang<sup>a</sup>, Lingyan Liu<sup>b</sup>, Peng Wei<sup>b,\*</sup>, Wei Feng<sup>a,\*</sup>, Tao Yi<sup>b,\*</sup>

<sup>a</sup> Department of Chemistry, Fudan University, Shanghai 200438, China

<sup>b</sup> State Key Laboratory for Modification of Chemical Fibers and Polymer Materials, Shanghai Engineering Research Center of Nano-Biomaterials and Regenerative Medicine, College of Chemistry and Chemical Engineering, Donghua University, Shanghai 201620, China

## ARTICLE INFO

### Article history:

Received 4 February 2024

Revised 3 June 2024

Accepted 14 June 2024

Available online 14 June 2024

### Keywords:

ROS

Aldehyde

Fluorescence

Methylene blue

Proximity tagging strategy

## ABSTRACT

Utilizing small molecules as markers for specific cells or organs within biosystems is a crucial approach for studying and regulating physiological processes. However, current tagging strategies, due to the presence of exposed highly reactive groups, suffer from drawbacks such as low tagging efficiency or insufficient spatial specificity, thereby diminishing their expected effectiveness. Consequently, there is a pressing need to develop a strategy capable of *in situ* labeling of active groups in response to cellular or *in vivo* stimuli, ensuring both high tagging efficiency and spatial specificity. In this work, we devised a strategy for releasing aldehyde groups activated by hypochlorous acid (HOCl). Compounds synthesized through this strategy can release the fluorophore methylene blue (MB) and aldehyde-based compounds upon HOCl activation. Given high reactivity of the released aldehyde group, it can effectively interact with macromolecules in biological systems, facilitating tagging and enabling prolonged imaging. To validate this concept, we further incorporated a naphthalimide structure with stable light emission to create **SW-110**. **SW-110** can specifically respond to *in vitro* and endogenous HOCl, when release MB, it also releases naphthalimide fluorophore with highly reactive aldehyde group for tagging within cells. This strategy provides a simple but efficient strategy for proximity tagging *in situ*.

© 2025 Published by Elsevier B.V. on behalf of Chinese Chemical Society and Institute of Materia Medica, Chinese Academy of Medical Sciences.

The utilization of small organic molecules for tagging cells and living organisms, followed by subsequent analysis of the tagging signals through techniques like fluorescence, mass spectrometry, is a common approach to investigate vital processes. Various methods have been employed in small organic molecule tagging strategies, including ligand-redirecting [1], covalent ligand directed release [2,3], lysine-reacting peptides [4], aptamer-based affinity labelling [5-8]. However, these methods come with their respective drawbacks and limitations. For instance, to achieve rapid responses, tagging molecules are often designed with highly active functional groups like aldehyde group or sulfhydryl groups. Unfortunately, such designs can introduce issues such as instability, low tagging efficiency, and poor specificity. Ideally, achieving the precise release of the tagging molecule at the desired target location would minimize these shortcomings and enhance the spatial specificity. However, achieving directional release of highly reactive functional groups under physiological conditions remains a chal-

lenge due to the lack of effective release strategies. Therefore, it is of high necessity to develop highly active functional group releasing strategies under physiological conditions for the design of proximity tagging probes.

Aldehyde group stands out as one of the prevalent and reactive functional groups. As mild electrophilic reagents, aldehydes exhibit unique reactivity. They can participate in bioorthogonal reactions for tagging [9-15], contribute to therapeutic hydrogel formation for wound healing [16-22], be coupled with amino residues for regulating physiological activities [23-25], for the synthesis of drugs [26-28], or for diseases treatment and antibacterial applications [29-34]. Due to their high reactivity, aldehyde groups serve as an ideal functional group for labelling. Nevertheless, the strategy for *in situ* activation and release of aldehyde groups remains unreported, primarily due to the high reactivity of aldehydes and the harsh reaction conditions required for their formation [35-38]. Given the widespread applications and importance of those compounds containing aldehyde groups, it is imperative to develop more effective methods for the *in situ* generation of aldehyde groups within organisms.

Reactive oxygen species (ROS) play a pivotal role in various biological processes, encompassing signal transduction, inflammation,

\* Corresponding authors.

E-mail addresses: [weipeng@dhu.edu.cn](mailto:weipeng@dhu.edu.cn) (P. Wei), [fengweifd@fudan.edu.cn](mailto:fengweifd@fudan.edu.cn) (W. Feng), [yitao@dhu.edu.cn](mailto:yitao@dhu.edu.cn) (T. Yi).

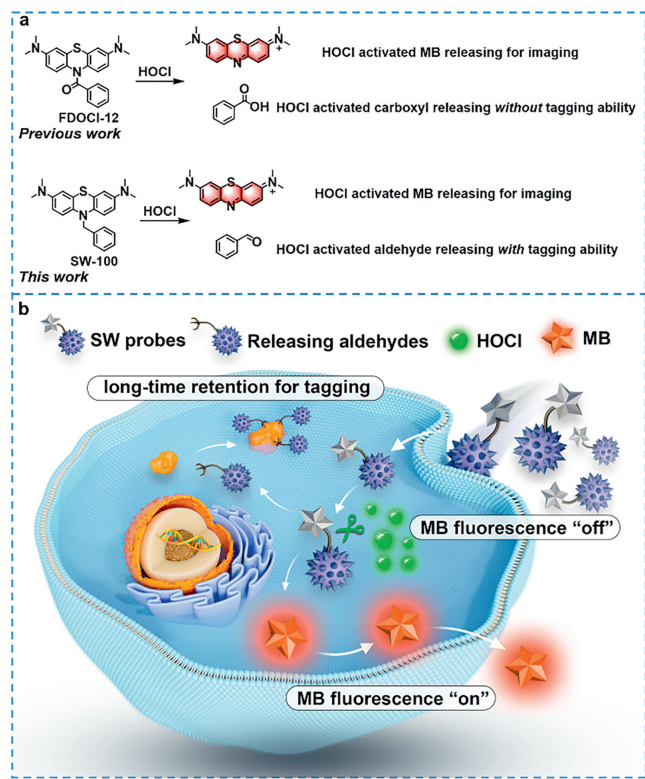


**Fig. 1.** (a) Previously reported HOCl-activated carboxyl release probe **FDOCI-12** and the designed HOCl-activated aldehyde release probe **SW-100** in this work. (b) The proposed mechanism of HOCl-activated aldehyde release within cells for tagging application.

and the pathological pathways of serious ailments such as cancer [39–42], kidney injury [43,44], liver damage [45–48], cardiovascular diseases [49–51] and neurodegenerative diseases [52–55]. Consequently, ROS have garnered significant attention in recent years, with increasing research exploring their potential as activators for prodrugs [56–58]. We have also successfully developed various types of prodrugs utilizing ROS as the activator based on the methylene blue (MB) structure, a widely used near-infrared (NIR) fluorescent dye, and an FDA-approved photodynamic drug [59–64].

In our earlier research, we successfully synthesized a series of leucomethylene blue (LMB) derivatives containing amide bonds. These compounds could be activated by HOCl to release carboxyl compounds (e.g., **FDOCI-12** in Fig. 1a). This observation prompted us to investigate whether a similar response would happen if the carbonyl group was directly replaced with an alkyl group, realizing the release of aldehyde in a mild condition. Actually, the oxidation of methylene-amino structures to aldehyde groups generally needs the help of metal catalysts [35] or enzymes [65], which is not benefit for its application in physiological conditions. It was excited to know that ROS could oxidize and break the carbon-nitrogen bonds between tertiary amines attached to phenol [66–69] or benzyl [70]. Since LMB happens to have an easily functionalized active nitrogen atom whose binding groups determine their ROS stimulation performance and the released molecular type (Fig. 1a), an aldehyde group release strategy activated by HOCl may be discovered via an ingenious structural design. We therefore designed MB-benzyl derivatives **SW-100** based on LMB at first (Fig. 1a). It was exciting that **SW-100** could release benzaldehyde under physiological conditions activated by HOCl. Multiple types of probes were thus developed based on this strategy (Scheme 1). All these compounds could release aldehyde groups in the presence of HOCl to some extent. Our research confirmed the universality of the strategy

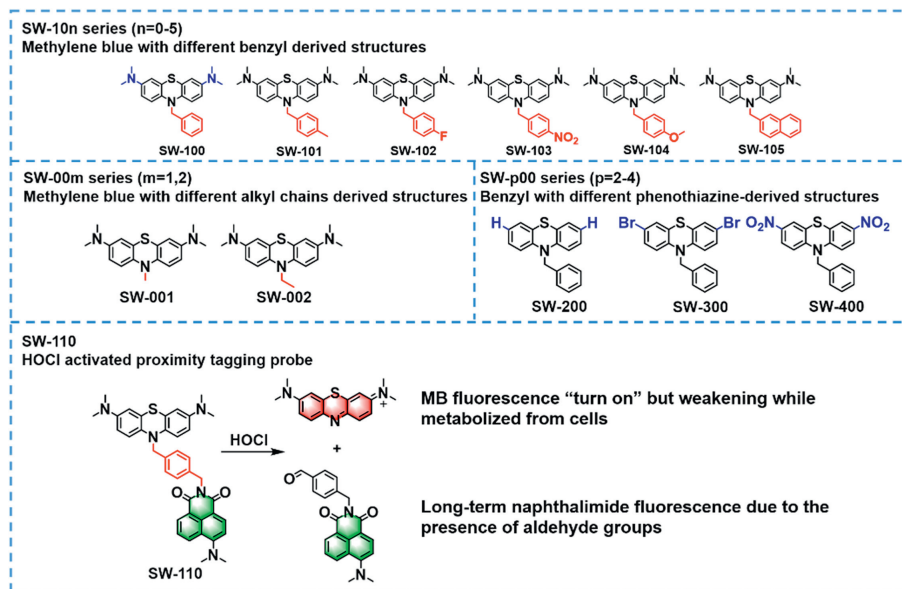
and elucidated the extent to which the strategy could be adapted. Following the activation of the probe, the released benzaldehyde group could be subsequently anchored within the cell. This further illustrated that the new proximity tagging strategy could be successfully used at the cellular level (Fig. 1b).

The synthesis details of **SW-100** were shown in Scheme S1 (Supporting information). HOCl could effectively activate **SW-100**. With the addition of HOCl from 0 to 10  $\mu\text{mol/L}$ , the fluorescent emission at 686 nm and the absorption at 664 nm of the probe (5  $\mu\text{mol/L}$ ) increased significantly, showing good HOCl responses and linear dependence on the concentration of HOCl in the range of 0–5  $\mu\text{mol/L}$  (Figs. 2a and b). Colour changes of **SW-100** (5  $\mu\text{mol/L}$ ) after adding different concentrations of HOCl were noticeable as well (Fig. S1 in Supporting information). The MALDI-TOF analysis of the response substance right after adding HOCl in the solution of **SW-100** verified the generation of LMB which would be quickly autoxidized to MB (Fig. S2 in Supporting information). The emission of MB could thus be used to track the reaction process of the probe.

**SW-100** displayed remarkable reaction sensitivity toward HOCl that could react with HOCl within 10 min with a low detection limit of 0.03  $\mu\text{mol/L}$  (Figs. 2c and d). Other types of ROS, including  $\text{H}_2\text{O}_2$ , TBHP,  $\text{ROO}^\bullet$ , NO,  $\text{KO}_2$ ,  $\text{ONOO}^-$ ,  $^\bullet\text{OH}$  and TBO $^\bullet$  caused negligible fluorescent intensity and colour changes compared to HOCl (Fig. 2e and Fig. S3 in Supporting information). Meanwhile, some commonly available anions, cations, and amino acids under physiological conditions, including  $\text{CH}_3\text{COO}^-$ ,  $\text{CO}_3^{2-}$ ,  $\text{SO}_4^{2-}$ ,  $\text{F}^-$ ,  $\text{Cl}^-$ ,  $\text{NO}_3^-$ ,  $\text{S}_2\text{O}_3^{2-}$ ,  $\text{ClO}_4^-$ ,  $\text{NH}_4^+$ ,  $\text{Na}^+$ ,  $\text{Mg}^{2+}$ ,  $\text{Al}^{3+}$ ,  $\text{K}^+$ ,  $\text{Ca}^{2+}$ ,  $\text{Fe}^{3+}$ ,  $\text{Cu}^{2+}$ ,  $\text{Ni}^{2+}$ , Tyr, Gly, Phe, Met, Leu, Arg, Pro, Lys, Gln, Glu, Asn, Ile, Asp, Val, His, Ser, Ala, Thr, Cys, Trp, could not cause remarkable fluorescence changes of **SW-100** (Fig. S4 in Supporting information). All these data showed that **SW-100** could react with HOCl with high efficiency and selectivity.

Since our goal was to investigate an activatable probe that could release aldehyde group for tagging biomolecules, it was the critical point to verify the generation of aldehyde and its coupling ability with other molecules. HPLC analysis of the reaction substances between **SW-100** and HOCl showed that one of the productions shared the same retention time with the benzaldehyde standard sample (5.16 min), indicating the producing of benzaldehyde (Fig. 2f). In addition, we used DCM to extract and enrich the production of the reaction between **SW-100** and HOCl, following by GC–MS analysis to identify the benzaldehyde generated after the reaction. (Fig. S5 in Supporting information). The proximity tagging performance of the generated benzaldehyde was thus investigated by adding aniline to the reaction system 30 min after their reaction. The existence of hydrazine compounds ((*E*)-*N*,1-diphenylmethanimine) formed by the coupling of benzaldehyde and aniline was successfully demonstrated (Fig. 2g). These data illustrated that **SW-100** could release benzaldehyde after activation by HOCl and the generated benzaldehyde could further react with amine group under physiological conditions *in situ*.

To verify that the activatable behavior of **SW-100** towards HOCl was not accidental, we further designed and synthesized the series of **SW-00m** ( $m = 1, 2$ ) and **SW-10n** ( $n = 1–5$ ) compounds with different alkyl chains and counterpointed group-derived benzyls, respectively, based on the LMB structure (Scheme 1, Schemes S1 and S2 in Supporting information). Their spectral properties activated by HOCl were investigated by fluorescence spectroscopy in PB (pH 7.4). With the addition of HOCl, the fluorescent emission at 686 nm of all these probes (5  $\mu\text{mol/L}$ ) increased significantly, showing good HOCl responses and linear dependence on the concentration of HOCl (Figs. S6–S13 in Supporting information). To verify the selectivity of **SW-00m** and **SW-10n** series probes towards ROS, the effects of different ROS (HOCl,  $\text{H}_2\text{O}_2$ , TBHP,  $\text{ROO}^\bullet$ , NO,  $\text{KO}_2$ ,  $\text{ONOO}^-$ ,  $^\bullet\text{OH}$ , TBO $^\bullet$ ) were measured through the fluorescence spectra of MB.



Scheme 1. Chemical structures of the series of HOCl-activated probes.

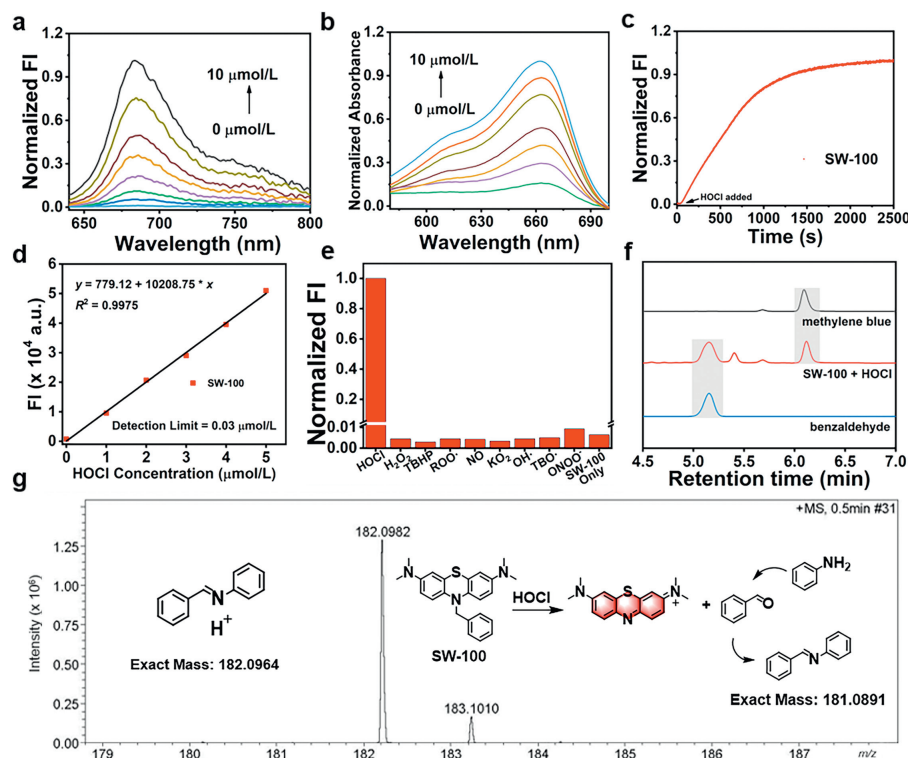


**Fig. 2.** ROS responsive properties of **SW-100**. (a) Normalized fluorescence and (b) absorption spectra of **SW-100** (5  $\mu\text{mol/L}$  in PB, pH 7.4) in the presence of different concentrations of HOCl (0–10  $\mu\text{mol/L}$ ). (c) Time-dependent changes in the fluorescence intensity of **SW-100** (5  $\mu\text{mol/L}$ ) at 686 nm after adding HOCl (15  $\mu\text{mol/L}$ ). (d) The linear relationship between the fluorescence intensity at 686 nm of **SW-100** and the concentration of HOCl (the detection limit is included). (e) Fluorescence intensity of **SW-100** (5  $\mu\text{mol/L}$  in PB, pH 7.4) at 686 nm after adding various ROS (from left to right: HOCl (10  $\mu\text{mol/L}$ ),  $\text{H}_2\text{O}_2$ , TBHP,  $\text{ROO}^\cdot$ , NO,  $\text{KO}_2$ ,  $\text{ONOO}^\cdot$ ,  $\cdot\text{OH}$ , TBO) with concentration of 100  $\mu\text{mol/L}$ . (f) HPLC analysis of the reaction of 5  $\mu\text{mol/L}$  **SW-100** with 15  $\mu\text{mol/L}$  HOCl (254 nm). (g) The HRMS spectra of (*E*)-*N*,1-diphenylmethanimine produced by benzaldehyde condensation with aniline.

The result showed that only HOCl induced a significant fluorescence enhancement of the probes. Other ROS had only minimal effects, indicating that the probes all had good selectivity for HOCl (Figs. S14–S21 in Supporting information).

Four probes, **SW-002** with alkyl chain, **SW-101**, **SW-103**, and **SW-104** containing benzene ring with no obvious push-pull electron effector group, electrophilic group and nucleophilic group on

the para-position, respectively, were selected to study their kinetics in response to HOCl (Fig. 3a). The time-dependent fluorescence changes of these probes showed a positive relationship between reaction rates and electrophilic properties of groups on benzene of the probes (Figs. S22–S25 in Supporting information). It was worth noting that although these derivatization structures could respond to HOCl and produce aldehyde-based compounds, the reaction de-

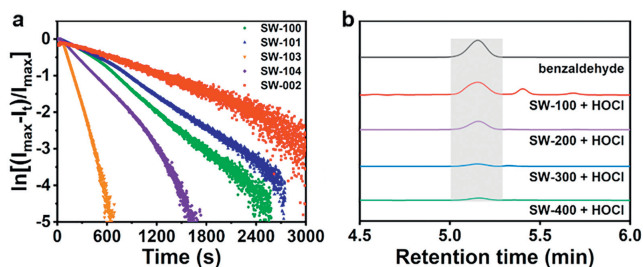


**Fig. 3.** (a) Pseudo-first-order kinetic plot of the reaction of 5  $\mu\text{mol/L}$  probes (**SW-002**, **SW-100**, **SW-101**, **SW-103**, **SW-104**) to 15  $\mu\text{mol/L}$  HOCl. (b) HPLC analysis of the reaction of 5  $\mu\text{mol/L}$  different probes (**SW-100**, **SW-200**, **SW-300**, **SW-400**) to HOCl (15  $\mu\text{mol/L}$ ) and standard compound benzaldehyde (254 nm).

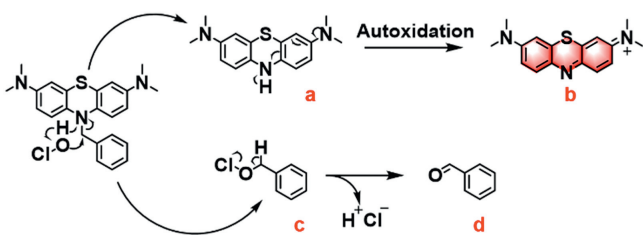


**Fig. 4.** Proposed reaction mechanism of the probes (**SW-100** as example) activated by HOCl releasing aldehyde-based compound and MB.

gree was not the same (Fig. S26 in Supporting information). An increase of the fluorescent intensity at 686 nm of **SW-103** (5  $\mu\text{mol/L}$ ) reached a plateau within only 7 min, which was the fastest one among the four probes upon adding HOCl (15  $\mu\text{mol/L}$ ). HPLC was used to determine the releasing rates of MB of the probes responding to HOCl according to the MB standard curve (Fig. S27 and Table S1 in Supporting information). The reaction of **SW-103** was most efficient with HOCl whose MB releasing efficiency came out to be 40.77%, consistent with the reaction kinetics.

To study the effect of the substituent of the aromatic structure of MB on the aldehyde group releasing process, we prepared three different phenothiazine-derived structures (the series of **SW-p00** ( $p=2-4$ ), Schemes S3-S5 in Supporting information) and investigated their response products after activated by HOCl through HPLC. Considerable benzaldehyde product was found in the reaction systems of **SW-100** and **SW-200**, whereas the generation of benzaldehyde in **SW-300** and **SW-400** was almost negligible (Fig. 3b), indicating that the structure of phenothiazine derivatives also played an important role on the release of aldehyde after stimulated with HOCl. The results showed that phenothiazine-derivatives with electron-donating groups (**SW-100**) were easier to react with HOCl than those containing electron-withdrawing groups (**SW-400**). The benzaldehyde release efficiency of **SW-100** was much higher than other benzyl derivatives of phenothiazine-derived structure (Table S2 in Supporting information).

After confirmed the response behavior of this series of molecules, we further studied the possible reaction mechanism. Since these probes only responded specifically to HOCl among the ROS and released aldehyde-group substances, the possible reaction mechanism was proposed as shown in Fig. 4. Taking **SW-100** as an example, due to high electronegativity, the tertiary amine N atom on LMB derivative has a relatively larger electron cloud density relative to the C atom on the methylene group of the benzyl. The H proton in HOCl tend to bind to the N atom, while the oxygen atom in  $[\text{ClO}]^-$  structure may attack methylene on the benzyl group. The transfer of electrons causes the C-N bond breaking to form unstable LMB (a), which has been verified byaldi-TOF

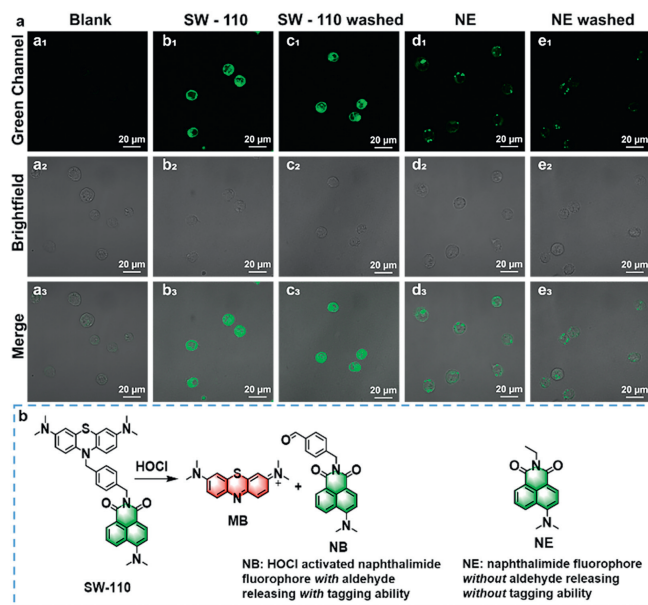


**Fig. 5.** (a) CLSM images of HL-60 cells incubated with **SW-110** (10  $\mu\text{mol/L}$ ) and **NE** (10  $\mu\text{mol/L}$ ) while one of each group of cells were washed by PBS every 6 h for 24 h.  $\lambda_{\text{em}} = 540 \pm 60 \text{ nm}$ ,  $\lambda_{\text{ex}} = 405 \text{ nm}$ . Scale bar = 20  $\mu\text{m}$ . (b) **SW-110** reacted with HOCl to exhibit two kinds of fluorescence.

analysis of the response substance right after adding HOCl into the solution of **SW-100** (Fig. S3), and benzyl hypochlorite structures (c). LMB spontaneously oxidizes to produce MB (b) that could be confirmed not only by its fluorescence but also by naked eye under visual light. The unstable benzyl hypochlorite structure undergoes intramolecular electron transfer, shedding  $\text{Cl}^-$  and  $\text{H}^+$  to form benzaldehyde (d). The proposed reaction mechanism is consistent with the structure-activity relationship of the probes, in which the electron-withdrawing group linked to the para position of benzyl (**SW-10n** ( $n=0-5$ ) series) and the electron-donating group on aromatic phenothiazine (**SW-p00** ( $p=1-4$ ) series) promote the reaction process.

The above results demonstrated that probes of **SW** series could release aldehydes in the presence of HOCl. The data also confirmed the universality of the strategy, which could be applied for the development of multiple types of probes. Further, we explored the feasibility of this aldehyde releasing strategy at the cellular level. Considering that the released aldehyde without fluorescence is difficult to be verified in cells, on the basis of **SW-100**, we introduced 4-*N,N*-dimethylamino-1,8-naphthalimide group with constant bright fluorescence at the para-position of the benzene ring and synthesized the probe **SW-110**. The synthesis details of **SW-110** were shown in Scheme S6 (Supporting information). **SW-110** was also verified to have good selectivity for HOCl, compared to commonly available anions, cations, and amino acids under physiological conditions (Fig. S28 in Supporting information). Compared to MB, which is well soluble in water and easily metabolized from intracellular, resulting in reduced fluorescence, naphthalimide fluorophores with aldehyde groups could be subsequently anchored within the cell and maintain long-term fluorescence after multiple times of washing. We thus used the fluorescence of MB and 4-((6-(dimethylamino)-1,3-dioxo-1*H*-benzo[*de*]isoquinolin-2(3*H*)-yl)methyl)benzaldehyde (**NB**) to indicate the reaction behavior of **SW-110** by confocal laser scanning microscopy (CLSM) (Fig. 5a). Fluorescence signal of MB in 633 nm channel was found in HL-60 cells after incubation of the probe, indicating that the probe could be activated by endogenous HOCl under physiological conditions, while the constantly bright fluorophore of **NB** indicated the

path and positioning of the probe. This further illustrated that the new proximity tagging strategy could be successfully used at the cellular level (Fig. 1b).

To verify the released NB containing an aldehyde part after reaction with HOCl had a better intracellular retention over the 4-*N,N*-dimethylamino-1,8-naphthalimide without an aldehyde group (**NE**), we compared the fluorescence decrease of different groups of cells incubated with **SW-110** (10 μmol/L) and **NE** (10 μmol/L) for 12 h on green and red channels before and after the cells were washed by PBS every 6 h for 24 h. CLSM images of HL-60 cells loaded with **SW-110** showed both green and red fluorescence, confirming the capability of **SW-110** to be activated by endogenous HOCl in living cells. After 24 h of washing, the fluorescence of MB could barely be observed while the fluorescence of **NB** remained basically unchanged (Fig. 5b and Fig. S29 in Supporting information). Comparing to the fluorescent signal of **NB**, the fluorescent intensity of **NE** showed an obvious weakening (Fig. 5b) which proved that **NB** with an aldehyde group retained better in cells than **NE**, attributed to aldehyde group's tagging ability. CLSM images of HL-60 cells loaded with both **SW-110** and NAC (500 μmol/L) showed only green fluorescence, proving the vital role of ROS in the progress of C–N bond cleavage and MB releasing (Fig. S30 in Supporting information). Cytotoxicity of **SW-110** were studied on HL-60 using MTT method, which showed low cytotoxicity of **SW-110** on HL-60 at experimental concentration (Fig. S31 in Supporting information).

In summary, we developed a novel HOCl-activated aldehyde group-releasing proximity-tagging strategy. Based on this strategy, a series of probes were designed, which performed good sensitivity and selectivity towards HOCl in aqueous solution and intracellular physiological conditions. These probes could release tagging-use benzaldehyde and its derivatives, while their proximity tagging ability in aqueous solution was demonstrated through aniline conjugation. The mechanism of the benzaldehyde release was proposed *via* the structure-activity relationship study. Furthermore, the activation and tagging capability of those probes on the cellular level was verified by using probe **SW-110** with double fluorescent signals. Our work provides a simple but efficient strategy for proximity tagging *in situ*. Further studies for the release of aldehyde groups in specific cellular organ and the application of the physiological-condition-aldehyde-releasing strategy *in vivo* are under way in our laboratory.

### Declaration of competing interest

The authors declare that they have no known competing financial interests or personal relationships that could have appeared to influence the work reported in this paper.

### CRediT authorship contribution statement

**Mengfan Zhang:** Conceptualization, Data curation, Formal analysis, Investigation, Methodology, Resources, Validation, Visualization, Writing – original draft. **Lingyan Liu:** Data curation, Investigation, Methodology, Resources, Software, Validation, Visualization, Writing – original draft. **Peng Wei:** Conceptualization, Data curation, Funding acquisition, Investigation, Methodology, Supervision, Validation, Visualization, Writing – original draft. **Wei Feng:** Conceptualization, Data curation, Investigation, Methodology, Supervision, Validation, Visualization, Writing – review & editing. **Tao Yi:** Conceptualization, Data curation, Funding acquisition, Investigation, Methodology, Project administration, Supervision, Validation, Visualization, Writing – review & editing.

### Acknowledgments

This study was financially supported by the National Natural Science Foundation of China (Nos. 22177019, 22377010, 22371038) and State Key Laboratory for Modification of Chemical Fibers and Polymer Materials (No. KF2206).

### Supplementary materials

Supplementary material associated with this article can be found, in the online version, at doi:10.1016/j.ccllet.2024.110127.

### References

- [1] T. Tamura, I. Hamachi, *J. Am. Chem. Soc.* 141 (2019) 2782–2799.
- [2] R.N. Reddi, E. Resnick, A. Rogel, et al., *J. Am. Chem. Soc.* 143 (2021) 4979–4992.
- [3] R.N. Reddi, A. Rogel, E. Resnick, et al., *J. Am. Chem. Soc.* 143 (2021) 20095–20108.
- [4] Y. Zhang, Y. Liang, F. Huang, et al., *Biochemistry* 58 (2019) 1010–1018.
- [5] C. Cui, H. Zhang, R. Wang, et al., *Angew. Chem. Int. Ed.* 56 (2017) 11954–11957.
- [6] Y. Tivon, G. Falcone, A. Deiters, *Angew. Chem. Int. Ed.* 60 (2021) 15899–15904.
- [7] J.L. Vinkenborg, G. Mayer, M. Famulok, *Angew. Chem. Int. Ed.* 51 (2012) 9176–9180.
- [8] Z. Xiang, H. Ren, Y.S. Hu, et al., *Nat. Methods* 10 (2013) 885–888.
- [9] S.R. Adusumalli, D.G. Rawale, K. Thakur, et al., *Angew. Chem. Int. Ed.* 59 (2020) 10332–10336.
- [10] A.K. Hurben, P. Ge, J.L. Bouchard, T.M. Doran, N.Y. Tretyakova, *Chem. Commun.* 58 (2022) 855–858.
- [11] Y. Guo, J. Tao, Y. Li, et al., *J. Am. Chem. Soc.* 142 (2020) 7404–7412.
- [12] H. Liu, X. Wei, Y. Nie, et al., *LWT-Food Sci. Technol.* 155 (2022) 112977.
- [13] Y. Zhang, M. Ucuncu, A. Gambardella, et al., *J. Am. Chem. Soc.* 142 (2020) 21615–21621.
- [14] M. Wolter, D. Valenti, P.J. Cossar, et al., *Angew. Chem. Int. Ed.* 59 (2020) 21520–21524.
- [15] P.J. Cossar, M. Wolter, L. van Dijk, et al., *J. Am. Chem. Soc.* 143 (2021) 8454–8464.
- [16] Y. Liang, Z. Li, Y. Huang, R. Yu, B. Guo, *ACS Nano* 15 (2021) 7078–7093.
- [17] W. Zhang, B. Bao, F. Jiang, et al., *Adv. Mater.* 33 (2021) 2105667.
- [18] M. Wu, J. Chen, W. Huang, et al., *Biomacromolecules* 21 (2020) 2409–2420.
- [19] R. Heras-Mozos, R. Gavara, P. Hernández-Muñoz, *Carbohydr. Polym.* 283 (2022) 119137.
- [20] Y. Guo, M. Wang, Q. Liu, et al., *Theranostics* 13 (2023) 161–196.
- [21] W. Chen, Y. Ming, M. Wang, et al., *Macromol. Rapid Comm.* 44 (2023) e2300128.
- [22] F.Y. Chung, Y.Z. Lin, C.R. Huang, K.W. Huang, Y.F. Chen, *Int. J. Biol. Macromol.* 255 (2024) 127947.
- [23] M. Wang, F.A. Dingler, K.J. Patel, *Blood* 139 (2022) 2119–2129.
- [24] J.M. Garlick, S.M. Sturlis, P.A. Bruno, et al., *J. Am. Chem. Soc.* 143 (2021) 9297–9302.
- [25] H.Y. Wang, Y. Zhang, M. Zhang, Y.Q. Zhang, *Int. J. Biol. Macromol.* 259 (2024) 129099.
- [26] V. Dhayalan, *Mini-Rev. Org. Chem.* 20 (2023) 593–611.
- [27] A.N. Fajer, H.A. Al-Bahrani, A.A.H. Kadhum, M. Kazemi, *J. Mol. Struct.* 1296 (2024) 136800.
- [28] Y. Liu, Z. Fu, H. Dong, et al., *Angew. Chem. Int. Ed.* 62 (2023) e202300906.
- [29] E. Uhl, F. Wolff, S. Mangal, H. Dube, E. Zanin, *Angew. Chem. Int. Ed.* 60 (2021) 1187–1196.
- [30] Y. Chen, Y. Liu, X. Hou, Z. Ye, C. Wang, *Chem. Res. Toxicol.* 32 (2019) 467–473.
- [31] S. Ma, W. Song, Y. Xu, et al., *Nano Lett.* 20 (2020) 2514–2521.
- [32] K. Wang, J. Li, Y. Yi, et al., *Nano Today* 42 (2022) 101355.
- [33] H. Gavilan, G.M.R. Rizzo, N. Silvestri, B.T. Mai, T. Pellegrino, *Nat. Protoc.* 18 (2023) 783–809.
- [34] R.E. Mohamed, M.A. Islam, *Chelonian Research Foundation* 18 (2023) 555–594.
- [35] R.L. Brabham, R.J. Spears, J. Walton, et al., *Chem. Commun.* 54 (2018) 1501–1504.
- [36] C. Wang, Y. Liu, C. Bao, et al., *Chem. Commun.* 56 (2020) 2264–2267.
- [37] A. Trachsel, N. Paret, D.L. Berthier, A. Herrmann, *ChemPhotoChem* 6 (2022) e202200045.
- [38] S. Azeez, P. Sureshbabu, S. Sabiah, J. Kandasamy, *Org. Biomol. Chem.* 20 (2022) 2048–2053.
- [39] G.Y. Liou, P. Storz, *Free Radic. Res.* 44 (2010) 479–496.
- [40] H. Nakamura, K. Takada, *Cancer Sci.* 112 (2021) 3945–3952.
- [41] B. Perillo, M. Di Donato, A. Pezone, et al., *Exp. Mol. Med.* 52 (2020) 192–203.
- [42] C.R. Reczek, N.S. Chandel, *Annu. Rev. Cancer Bio.* 1 (2017) 79–98.
- [43] M.V. Irazabal, V.E. Torres, *Cells* 9 (2020) 1342.
- [44] N. Xu, S. Jiang, P.B. Persson, et al., *Acta Physiol.* 229 (2020) e13477.
- [45] L. Conde de la Rosa, L. Goicoechea, S. Torres, C. Garcia-Ruiz, J.C. Fernandez-Checa, *Livers* 2 (2022) 283–314.
- [46] S. He, J. Song, J. Qu, Z. Cheng, *Chem. Soc. Rev.* 47 (2018) 4258–4278.
- [47] Y. Duan Kenry, B. Liu, *Adv. Mater.* 30 (2018) 1802394.

- [48] V. Sanchez-Valle, N.C. Chavez-Tapia, M. Uribe, N. Mendez-Sanchez, *Curr. Med. Chem.* 19 (2012) 4850–4860.
- [49] D. Moris, M. Spartalis, E. Spartalis, et al., *Ann. Transl. Med.* 5 (2017) 326.
- [50] N. Panth, K.R. Paudel, K. Parajuli, *Adv. Med.* 2016 (2016) 9152732.
- [51] J.N. Peoples, A. Saraf, N. Ghazal, T.T. Pham, J.Q. Kwong, *Exp. Mol. Med.* 51 (2019) 1–13.
- [52] G.H. Kim, J.E. Kim, S.J. Rhie, S. Yoon, *Exp. Neurobiol.* 24 (2015) 325–340.
- [53] E.O. Olufunmilayo, M.B. Gerke-Duncan, R.M.D. Holsinger, *Antioxidants* 12 (2023) 517.
- [54] A. Singh, R. Kukreti, L. Saso, S. Kukreti, *Molecules* 24 (2019) 1583.
- [55] Y. Zhou, Y. Zhen, G. Wang, B. Liu, *Front. Neuroanat.* 16 (2022) 910427.
- [56] X. Chen, F. Wang, J.Y. Hyun, et al., *Chem. Soc. Rev.* 45 (2016) 2976–3016.
- [57] C. Nathan, *J. Clin. Invest.* 111 (2003) 769–778.
- [58] Y. Yang, Q. Zhao, W. Feng, F. Li, *Chem. Rev.* 113 (2013) 192–270.
- [59] D. Liu, L. Liu, F. Liu, et al., *Adv. Sci.* 8 (2021) 2100074.
- [60] F. Liu, L. Liu, D. Liu, et al., *Chem. Sci.* 13 (2022) 10815–10823.
- [61] L. Liu, L. Jiang, W. Yuan, et al., *ACS Sensors* 5 (2020) 2457–2466.
- [62] L. Liu, F. Liu, D. Liu, et al., *Angew. Chem. Int. Ed.* 61 (2022) e202116807.
- [63] P. Wei, L. Liu, Y. Wen, et al., *Angew. Chem. Int. Ed.* 58 (2019) 4547–4551.
- [64] P. Wei, W. Yuan, F. Xue, et al., *Chem. Sci.* 9 (2018) 495–501.
- [65] N. Fan, C. Wu, Y. Zhou, et al., *Anal. Chem.* 93 (2021) 7110–7117.
- [66] J. Cheng, D. Li, M. Sun, et al., *Chem. Sci.* 11 (2020) 281–289.
- [67] T. Peng, X. Chen, L. Gao, et al., *Chem. Sci.* 7 (2016) 5407–5413.
- [68] Q. Sun, J. Xu, C. Ji, et al., *Anal. Chem.* 92 (2020) 4038–4045.
- [69] H. Zhang, J. Liu, Y.Q. Sun, et al., *Chem. Commun.* 51 (2015) 2721–2724.
- [70] M. Weber, H.H. Han, B.H. Li, et al., *Chem. Sci.* 11 (2020) 8567–8571.